Shifting to a 36-month fuel cycle with advanced moderating burnable absorbers enabling high assay low enriched uranium (HALEU)

Bolukbasi, Mustafa; Middleburgh, Simon; Vrtiska, Scott; Lee, Bill

Progress in Nuclear Energy

DOI:
10.1016/j.pnucene.2023.105011

Published: 01/03/2024

Publisher's PDF, also known as Version of record

Progress in Nuclear Energy 168 (2024) 105011

Contents lists available at ScienceDirect

Progress in Nuclear Energy

journal homepage: www.elsevier.com/locate/pnucene

Shifting to a 36-month fuel cycle with advanced moderating burnable absorbers enabling high assay low enriched uranium (HALEU)

M.J. Bolukbasi [a,*], S.C. Middleburgh [a], S. Vrtiska [b], W.E. Lee [a]

[a] Nuclear Futures Institute, Bangor University, Bangor, LL57 1UT, UK
[b] Westinghouse Electric Sweden, Västerås, 72163, Sweden

ARTICLE INFO

Keywords:
Burnable absorber
MDBAP
HALEU
Casmo-4/simulate-3
Advanced technology fuels

ABSTRACT

Meeting the increasing demand for energy requires more efficient and economical use of resources. Thus, extending the fuel cycle of nuclear reactors that commonly operate on 18-month cycles has become an important area of research both academically and industrially. However, longer fuel cycles necessitate higher fuel enrichment, which poses a greater challenge in terms of reactivity control. In this study, the operation and safety of nuclear power plants in 36-month fuel cycles using High Assay Low Enriched Uranium (HALEU) enriched up to 7.00 wt% were assessed. Moderated Discrete Burnable Absorber Pins (MDBAPs), containing ZrB_2 and UB_2 have the potential to improve fuel efficiency and fuel economy in long cycles, were introduced as a new burnable absorber solution. Comprehensive evaluations of MDBAPs were undertaken using fuel cycle analyses with the advanced Studsvik CASMO-4/SIMULATE-3 code system. This assessment focuses on understanding the impact of MDBAPs on several key aspects: reactivity feedback parameters, peaking factors, power distribution profiles, and shutdown margin. The results indicate that MDBAPs are a promising burnable absorber option for fuel enriched up to 7.00 wt% (HALEU), demonstrating substantial promise for supporting a 36-month fuel cycle while complying with those operational safety standards and limits.

1. Introduction

In an economic sense, the capacity factor of a Nuclear Power Plant (NPP) is important to its financial sustainability. Since the capital cost of an NPP is significant, a high-capacity factor can assist in offsetting this by increasing the amount of power generated. (Carlson et al., 2020). As such, a high-capacity factor can increase nuclear energy's economic competitiveness compared to other sources of energy generation.

Advanced technology fuel with high burnup can increase the capacity factor of nuclear reactors. The use of fuel that can reach high burnup can extend fuel cycle length and reduce the number of refuelling outages, thus increasing the capacity factor of the reactor (Stewart et al., 2021). The reduction in unplanned outages due to their improved robustness is also a compelling financial benefit for the industry.

Today's Light Water Reactors (LWRs), such as Pressurized Water Reactors (PWRs) and Boiling Water Reactors, are typically operated on 12-month and 18-month cycles (World Nuclear Association, 2021). Particularly for PWRs, numerous studies are being conducted to extend the cycle duration to 24-month and beyond. Furthermore, when examining Small Modular Reactors (SMRs), it is observed that a significant majority of them have fuel cycle lengths between 18 and 24-months (IAEA, 2020). Of course, being smaller and modular, SMRs offer flexibility, and their inherently longer cycle lengths compared to LWRs provide the advantage of having a higher capacity factor (Lokhov et al., 2013). Nevertheless, similar efforts are also being directed toward SMRs to enable core designs that would support even longer cycles.

Enrichment restrictions beyond 5.00 wt% of ^{235}U, have long been a limit for the commercial nuclear industry (Dias et al., 2019). Although these restrictions are in place to prevent the production of materials that could be used to manufacture a nuclear weapon, the limit also restricts the potential of nuclear energy to achieve higher burnups, improving fuel cycle economics. As the use of energy increases and the need for more efficient and sustainable energy sources becomes more important, there is growing interest in the development of fuel with higher enrichment levels.

The use of advanced technology fuel, with high-assay low-enriched uranium (HALEU), that is uranium enriched below 20 wt% ^{235}U, allows a reactor to achieve higher burnup and extract more energy from a given amount of fuel (Carlson et al., 2020). However, the use of HALEU, even at lower enrichment levels compared to the maximum 20 wt% (i.e. <7

* Corresponding author.
E-mail address: mbolukbasi@bangor.ac.uk (M.J. Bolukbasi).

https://doi.org/10.1016/j.pnucene.2023.105011
Received 27 March 2023; Received in revised form 19 October 2023; Accepted 6 December 2023
Available online 17 December 2023

wt% ^{235}U), reveals some challenges in terms of reactivity control within light water reactors. Reactivity control and the ability to safely shutdown after a long cycle lengths is a critical design factor, as it meets the high burnup requirements in terms of thermomechanical behaviour.

Burnable Absorbers (BAs) are an important feature used to maintain reactivity control and to avoid power peaks during the operation (Durazzo et al., 2018). Integral Fuel Burnable Absorbers (IFBAs) and Integral Burnable Absorbers (IBAs) are used extensively in today's LWRs. IFBAs, developed by Westinghouse Electric Company, are obtained by coating ZrB_2 on the surface of the fuel pellet in the form of a thin layer (Alameri and Alrwashdeh, 2021). IBAs, on the other hand, are a solution obtained by mixing a neutron-absorbing compound, usually Gd_2O_3 up to 14 wt%. (Papynov et al., 2020), with UO_2 fuel. Both designs are applied to a certain number of fuel rods within certain fuel assemblies to meet the needs of the reactor reactivity.

The composition of natural boron includes ^{10}B (19.9 wt%) and ^{11}B isotopes (Berglund and Wieser, 2011). The ^{10}B isotope, having a thermal neutron absorption cross-section of ~3800 b, undergoes a transformation during reactor operation. This transformation occurs due to the capture of neutrons, leading to the transmutation of ^{10}B into ^{7}Li and ^{4}He, as in Eq. (1). In addition, boron's residual neutron poisoning is lower compared to Gd (Burr et al., 2019).

$$ {}^{10}_{5}B + {}^{1}_{0}n \rightarrow {}^{7}_{3}Li + {}^{4}_{2}He + \gamma \qquad \text{(Eq. 1)} $$

On the other hand, despite the presence of isotopes with high thermal neutron absorbing cross-sections in Gd_2O_3 (^{155}Gd and ^{157}Gd), isotopes with low cross-sections lead to a residual reactivity penalty at the end of the fuel's life (EOL), displacing fuel and breeding of isotopes with some significant neutronic penalty. Additionally, increasing the Gd_2O_3 weight in the fuel composition leads to a decrease in the fuel's thermal conductivity (Dalle et al., 2013; Qin et al., 2020). As longer cycles can be achieved with a higher amount of fissile material, the requirement for a higher amount of BA would be a necessity and a higher ratio of Gd_2O_3 loading results in a higher residual reactivity penalty and a larger reduction in thermal conductivity. Although these negative effects can be somewhat eliminated by enriching the Gd_2O_3 with its main neutron absorber isotopes (Bolukbasi et al., 2023), its applicability for cycles exceeding 24-month with HALEU fuel is presently undetermined. IFBAs, on the other hand, cause very little in the way of a residual reactivity penalty, however, due to the relatively rapid depletion of ^{10}B isotopes in its composition, IFBAs are not suitable for cycles longer than 24-month (Choe et al., 2016; Dandi et al., 2020; Westinghouse Electric Company, 2018). Renier and Grossbeck stated that in IFBA usage scenarios, the ZrB_2 coating thickness can be increased only within certain limits and the self-shielding effect will be limited even at the maximum BA ratio in the reactor core since it is not depleted slowly enough (Renier and Grossbeck, 2001).

Alhattawi et al. investigated the possible cladding options for APR-1400 and concluded that Silicon Carbide (SiC) is a promising cladding option based on sensitivity analyses (Alhattawi et al., 2023). Additionally, Alrwashdeh and Alamer achieved a 24-month cycle by using IFBA on soluble-boron-free APR-1400 core in their study. They indicated that with the utilisation of SiC cladding with an additional IFBA layer, a 24-month cycle can be attained without impacting either the thermal neutron spectrum or radial power distribution, thus ensuring reactor safety and efficiency within a 24-month fuel cycle (Alrwashdeh and Alameri, 2023).

Conversely, UB_2 is being considered as a potential candidate for a burnable absorber. With its intermetallic structure, it has both high thermal conductivity and a high melting point compared to UO_2 (Kardoulaki et al., 2020). Due to its higher density compared to UO_2, it enables higher fissile isotope loading to the reactor core, suppresses reactivity at the beginning of the fuel's life, and enables higher reactivity at the end of the fuel's life (Burr et al., 2019). Considering these features, UB_2 shows itself as a candidate burnable absorber for reaching high burnup.

2. Designed model

The BA-pellet design, known as the Discrete Burnable Absorber Pin (DBAP), which was developed by (Enica et al., 2018) with the assistance of Westinghouse Electric Company, was studied by the authors of this article (Bolukbasi et al., 2022). In the study neutronic analyses were carried out to inform future studies and the potential of the design was revealed. In the design, burnable absorbers, such as ZrB_2 or UB_2, were not included in the fuel mixture in the manner of Gd_2O_3, but instead, were positioned as discrete burnable absorber pins within the annular fuel pellet. Overall, that study demonstrated that the utilisation of the DBAP as a burnable absorber can be implemented in an effective manner and has potential use in prolonged fuel cycles which require ^{235}U enrichment levels higher than 5.00 wt%.

Within the scope of the development studies of the design, it was determined that the beryllium oxide moderator addition to DBAP could pave the way for increasing the effective full power days (EFPD). The Moderated Discrete Burnable Absorber Pins' (MDBAPs') design is in the form of an annular BA with a moderator pin (beryllium oxide) in the centre inside the annular fuel pellet, as can be seen in Fig. 1. The incorporation of a moderator at the central location, leads to a decrease in the velocity of neutrons as in wet annular burnable absorbers (Evans et al., 2022). Therefore, their capability of being absorbed is enhanced. This mechanism facilitates the capture of an increased number of neutrons by the fissile isotopes present in the reactor pellet, and thus, promoting a greater number of fission reactions, leading to efficient utilisation of fuel, levelling the rate of fission of isotopes near the centre of the pellet as well as at the periphery (Insulander Björk and Kekkonen, 2015), and therefore results in an increase in the overall power output (Evans et al., 2022).

In this study, the transition from an 18-month fuel cycle utilizing IFBA as a burnable absorber to a 36-month fuel cycle incorporating ZrB_2 or UB_2 MDBAPs with UO_2 that has ^{235}U enrichment level beyond 5.00 wt %. was investigated. The operational safety and design parameters, including the moderator temperature coefficient and the shutdown margin (SDM), were taken into account and the benefits of implementing MDBAPs were evaluated.

3. Method

An advanced nuclear design code system: Studsvik CASMO-4/SIMULATE-3, was used to conduct fuel cycle simulations. A standard Westinghouse Electric Company designed 3-loop PWR reactor was selected as a reference Nuclear Power Plant (NPP) for the simulations. Table 1 provides the design parameters of the Westinghouse PWR and the parameters that were employed in the simulations.

In the scenario of IFBA usage, it was assumed that while 64 fresh fuel assemblies are loaded in each fuel cycle, 35 once-burned fuel assemblies and 29 twice-burned fuel assemblies are discharged every 508 EFPDs cycle. Delgado and others report that single-batch cores are known to be lacking in fuel-management flexibility compared to multi-batch cores. The reason for this is that the high reactivity of newly added fuel cannot

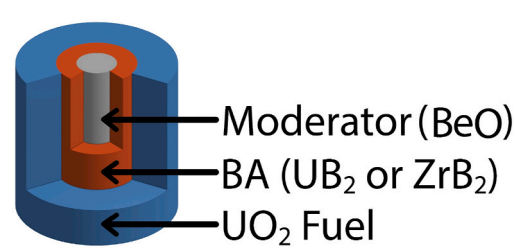

Fig. 1. MDBAP design.

Table 1
Fuel design parameters and operation limits of a standard Westinghouse 3-loop PWR (DiGiovine and Gheorghiu, 1999; Duke Energy, 2018; U.S.NRC, 1982).

Reactor Type	3-Loop PWR
Coolant temperature (°C)	286
Power Output (MWt/MWe)	2900/965
System pressure (MPa)	15.5
Control rod Material	Ag - In – Cd
Number of assemblies	157
Rod array	17 × 17
Assembly pin pitch (cm)	1.26
Fuel pellet radius (cm)	0.410
Number of control rods/guide tube	24/1
Number of BA rods	24
Fuel assembly pitch (cm)	21.50
Fuel assembly height (cm)	365.76
Cladding material	Zircaloy-4
UO_2 fuel density (% of TD)	95.5
ZrB_2 density (g/cm^3)	5.8
UB_2 density (g/cm^3)	12.12
Nuclear Enthalpy Rise Hot Channel Factor ($F_{\Delta H}$)	≤1.66
Heat Flux Hot Channel Factor (F_Q)	≤2.41
Moderator temperature coefficient (pcm/°F)	$-50 \leq$ MTC ≤ 0
Shutdown Margin (pcm)	≤ -1770
Cycle length/Effective full power days	18/508 – 36/1055
Refuelling outages (days)	40
IFBA loading (mg ^{10}B/cm)	0.772

be effectively balanced out by a lower reactivity of burned fuel assemblies (Garcia-Delgado et al., 1999). Furthermore, a single-batch core necessitates a higher load of burnable absorbers, adversely impacting neutron efficiency. This condition also results in lower burnup levels when contrasted with the outcomes of multi-batch loading strategies (Carelli and Ingersoll, 2014). For this reason, a two-batch loading strategy was chosen over single-batch loading for the simulations. The MDBAP usage scenarios, aiming at 1055 EFPDs cycle, were investigated by loading different numbers of the fresh fuel assemblies, in each fuel cycle. Upon initial utilisation, the assemblies which had undergone the least burnup were chosen and positioned in locations within the reactor core where maximum burning could occur for the subsequent cycle. In the scenarios of UB_2 usage as a burnable absorber, the uranium enrichment level of UB_2 was maintained in congruence with the enrichment level of UO_2 located in the same fuel assembly. Furthermore, it was assumed that both ZrB_2 and UB_2 burnable absorbers possessed a natural boron isotopic composition (i.e. no ^{10}B enrichment).

The two-group cross-section data production of fuel assemblies with varying enrichment levels for IFBA rods was performed on CASMO-4. Additionally, the two-group cross-section data production for fuel assemblies with dissimilar fuel enrichment levels, different radius MDBAP outer radii and moderator of MDBAP rods was executed. The required library for SIMULATE-3 was created using the CMS-Link software. In the scenario of IFBA usage, the determination of the required enrichment level to provide the design 508 EFPDs cycle was conducted by varying the enrichment level of the fuel groups 0.05 wt% within the range between 4.00 wt% and 4.95 wt%. Assuming a constant refuelling time, simulations were conducted to detect the number of fresh fuel assemblies, enrichment levels, MDBAP properties required to provide 1055 EFPD (i.e. a 36-month cycle), and the distribution of these fuel assemblies in the reactor core was performed. An enormous number of simulations, varying enrichment levels of ^{235}U (from 6.20 wt% to 6.85 wt%) and different types of BA and moderator radii (between 0.4 mm and 2.5 mm) were conducted in order to achieve the targeted EFPD. From the simulation results those candidates that were within the design and safety limits and exhibited the possible lowest initial Critical Boron Concentration (CBC) with the lowest possible ^{235}U enrichment level were chosen as the subject of examination in this paper.

The placement of fresh fuel assemblies in the reactor core is divided into four groups according to the enrichment level used in IFBA and MDBAP scenarios to avoid power peaks. Furthermore, a 15.24 cm BA-free zone on both the top and bottom of the fuel assembly was preferred in use in IFBA design 24 (Barsic et al., 2008; Elsawi and Hraiz, 2015), while 15. cm on top and 10.24 cm on bottom BA-free zones were preferred for the MDBAPs to achieve a flatter axial power distribution. Fig. 2 shows 112 fuel rod locations that include BA (Ames Ii et al., 2010) while the fuel loading layout for 18-month and 36-month fuel cycles can be seen in Fig. 3.

It is imperative that the fuel has to be within the design operational safety limits. Consequently, a thorough examination of various fuel parameters, including moderator temperature coefficient, Nuclear Enthalpy Rise Hot Channel Factor ($F_{\Delta H}$), Heat Flux Hot Channel Factor (F_Q), Isothermal Temperature Coefficient (ITC), Uniform Doppler Coefficient (UDC), and Boron Coefficient (BC), were carried out. Furthermore, the average axial relative power fraction profile and assembly-wise 2D relative power fraction of the fuel core were examined at 12 axial nodes.

All simulations were conducted under the conditions of Hot Full Power (HFP). Additionally, calculations were performed to assess the potential impact of MDBAPs on the SDM. The SDM was calculated using Eq. (2) (Hiscox, 2018), taking into account the following scenarios: the difference in reactivity values between HFP and Hot Zero Power (HZP), represented by Δk_1, the difference in reactivity values between HFP and All Control Rods In (ARI), represented by Δk_2, and the difference in reactivity values between ARI and the scenario in which the most effective control rod was not functional represented, by Δk_3.

$$SDM = \Delta k_1 + 0.9(\Delta k_2 - \Delta k_3) \quad \text{(Eq. 2)}$$

4. Results and discussion

In Fig. 4, the k_{inf} curves of DBAPs and MDBAPs employing different burnable absorbers (ZrB_2 in Fig. 4a and UB_2 in Fig. 4b) are compared with IFBA-equipped and BA-free fuel models to observe the difference in reactivities provided by these models. In this comparison, the DBAPs possess a radius of 1.2 mm. Furthermore, the MDBAPs also have a 1.2 mm radius, with one featuring a moderator radius of 1.0 mm while the other has a moderator radius of 0.6 mm. It is noteworthy that in the fuel models where IFBAs, DBAPs, and MDBAPs are employed, the applications of these BAs have been implemented on 112 fuel rods (as in Fig. 2). Furthermore, the behaviour of ^{10}B depletion behaviour these fuel models are provided in Fig. 5.

Upon examining Fig. 4, it is observed that there is a sharp decline at the beginning of the life (BOL) of each fuel model. The reason for this decline is the rapid reproduction of ^{149}Sm and ^{135}Xe atoms, which have

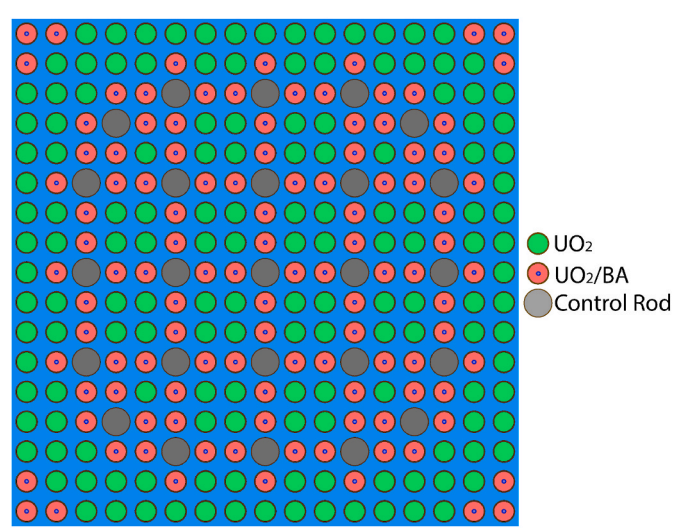

Fig. 2. Fuel assembly design with 112 IFBA or MDBAP rods (Ames Ii et al., 2010).

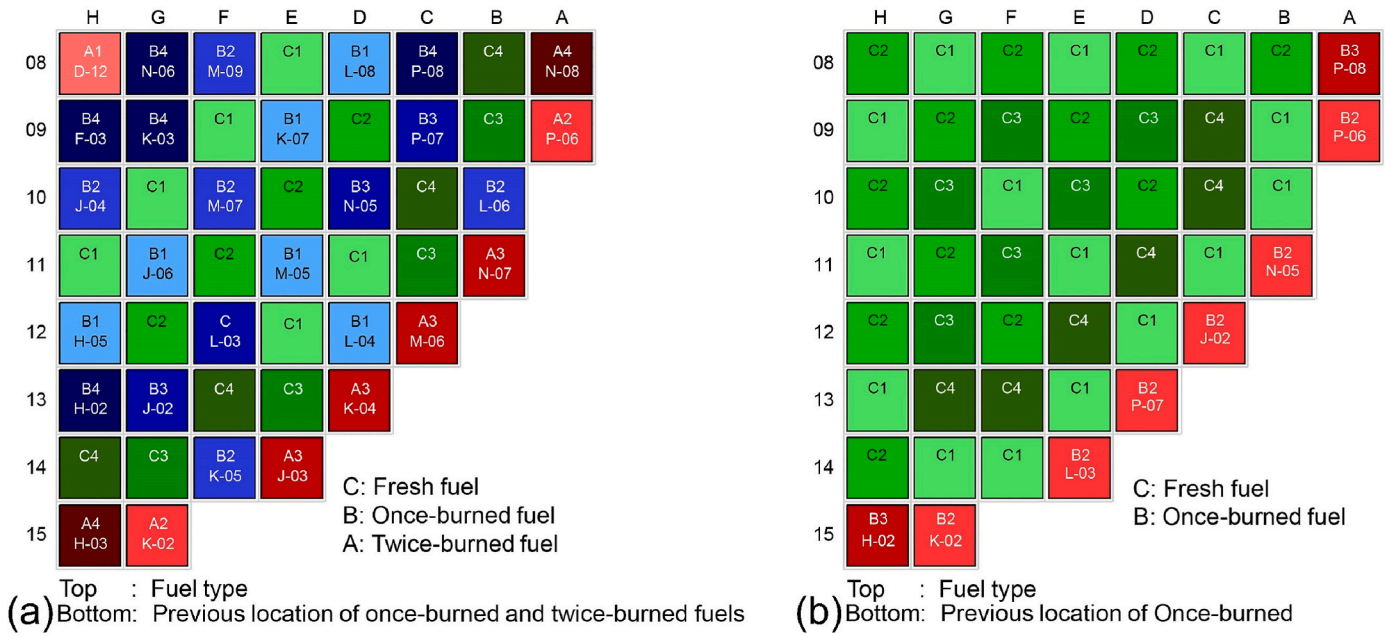

Fig. 3. Fuel loading layout of 18-month fuel cycle with IFBA (a) (Amjad et al., 2014) and 36-month fuel cycle with MDBAP (b).

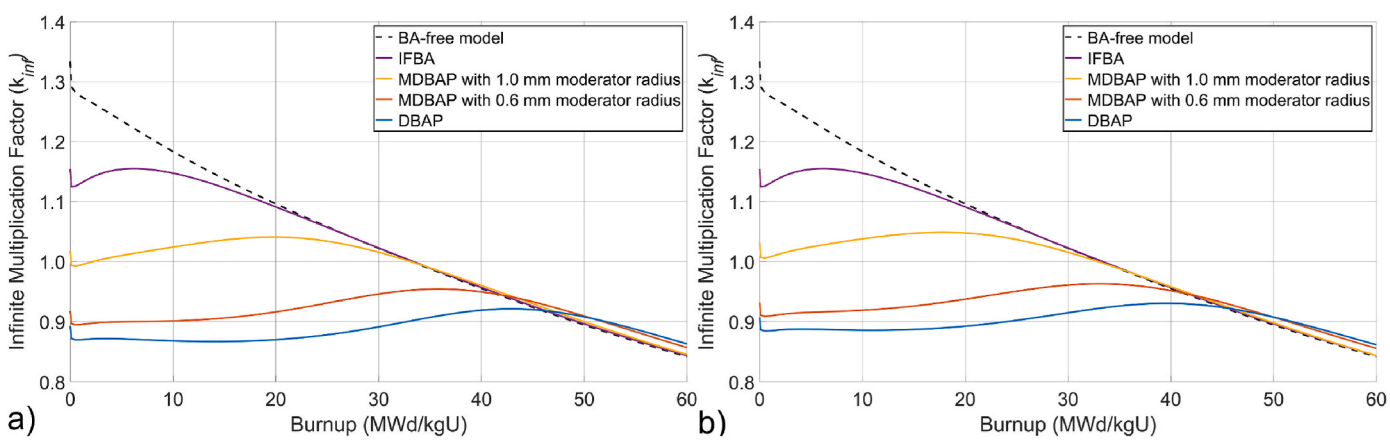

Fig. 4. Infinite multiplication factors of different fuel models.

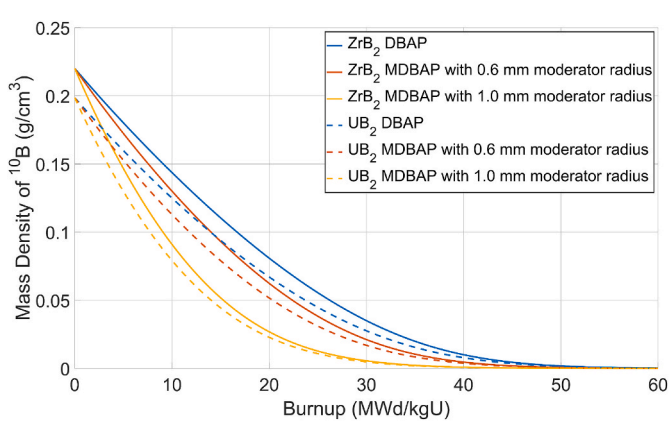

Fig. 5. ^{10}B depletion behaviour of different fuel models.

a high thermal neutron absorption cross-section (Attom et al., 2019). On the other hand, DBAPs and MDBAPs, possessing both types of BAs, have a lower k_{inf} value at the beginning of the lifespan compared to IFBA and BA-free fuel models.

When Fig. 4a is examined, it is found that the IFBA-equipped fuel model possesses an initial k_{inf} value that is approximately 17,955 pcm lower than that of the BA-free fuel model (1.15404 and 1.33359 respectively) at BOL. On the other hand, the ZrB_2 DBAP has a k_{inf} value of 0.89227 at BOL. However, with the utilisation of a moderator, the fuel model that has ZrB_2 MDBAPs shows a higher k_{inf} value than the ZrB_2 DBAP. Furthermore, the fuel model has ZrB_2 MDBAPs with a moderator radius of 0.6 mm shows a 2,530 pcm higher k_{inf} value than the ZrB_2 DBAPs at BOL. Similarly, the fuel model that has ZrB_2 MDBAP with a moderator radius of 1.0 mm exhibits a k_{inf} value that is 12,532 pcm higher than that of the ZrB_2 DBAP at BOL.

On the other hand, when compared with their counterparts that use UB_2 as the BA, the ZrB_2 DBAP, the ZrB_2 MDBAP with a 0.6 mm moderator radius, and the MDBAP with a 1.0 mm moderator radius display higher k_{inf} values at BOL. Specifically, the increases are 1497 pcm, 1443 pcm, and 1388 pcm, respectively.

An analysis of the behaviour throughout the lifetimes of fuel models reveals that after the depletion of the majority of the ^{10}B atoms within the system (see Fig. 6), k_{inf} values reach the peaks in all fuel models. In addition, fuel models containing MDBAPs with a 1.0 mm radius

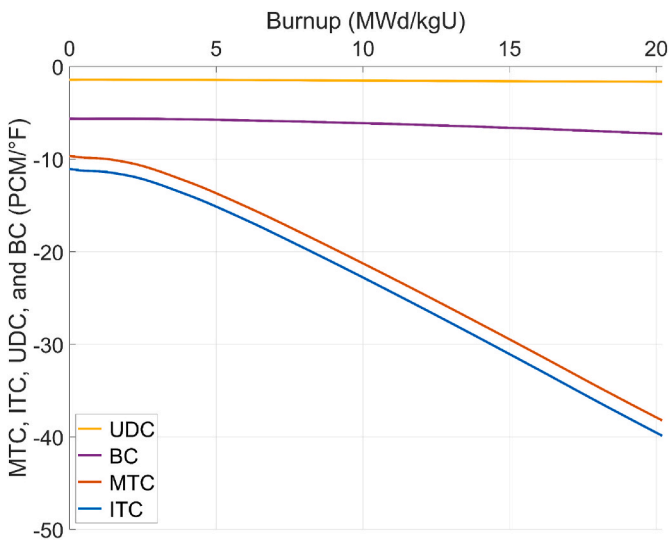

Fig. 6. Moderator temperature coefficient, isothermal temperature coefficient, uniform Doppler coefficient, and boron coefficient curves of 18-month equilibrium cycle with IFBA.

moderator reach this peak point earlier compared to those fuel models with a 0.6 mm radius moderator and those with DBAPs for both ZrB_2 and UB_2 usage cases.

Subsequently, fuel models utilizing ZrB_2 DBAPs and ZrB_2 MDBAPs demonstrate nearly identical k_{inf} values as the BA-free fuel model at approximately 46.00 MWd/kgU. From this point, they maintain higher k_{inf} values for the rest of their operational life. In contrast, fuel models that employ ZrB_2 MDBAPs and UB_2 MDBAPs with a 0.6 mm moderator radius intersect with the BA-free fuel model around 41.00 MWd/kgU, exhibit higher k_{inf} values for the remainder of their lifespan.

Lastly, fuel models featuring ZrB_2 MDBAPs and UB_2 MDBAPs with a 1.0 mm moderator radius achieve the same level as the BA-free fuel model at 33.00 MWd/kgU and 34.00 MWd/kgU, respectively. After reaching these points, they display higher k_{inf} values than the BA-free fuel model for the rest of their life.

On the other hand, when the k_{inf} values at EOL are compared, it is observed that all fuel models provide higher values than the BA-free fuel model. Specifically, when compared with the BA-free fuel model, the fuel model using IFBAs, the fuel model in which ZrB_2 DBAPs are used, the fuel model with ZrB_2 MDBAPs having a 0.6 mm moderator radius, and the fuel model with ZrB_2 MDBAPs possessing a 1.0 mm moderator radius, have higher k_{inf} values by 170 pcm, 2,155 pcm, 1,508 pcm, and 346 pcm, respectively. Additionally, it is noteworthy that, when fuel models containing ZrB_2 are compared with those containing UB_2, the ZrB_2-containing fuel models exhibit up to 140 pcm higher k_{inf} values at the end of their lifetimes.

Upon examining Fig. 5, it becomes apparent that fuel models containing both ZrB_2 and UB_2 exhibit a slower depletion behaviour of ^{10}B due to the self-shielding effect in DBAPs. However, with the addition of a moderator and an increase in the moderator's radius, consequently leading to an expansion in the absorber material's inner surface area, there is an observable acceleration in the ^{10}B depletion rate. Additionally, the stages at which ^{10}B atoms are almost entirely depleted are quite similar among fuel models with the same physical characteristics although they have different BA types.

From the results of various simulations, it was determined that 508 EFPDs could be achieved with different fuel loading options when IFBA was employed. Out of these options, the case with the lowest initial CBC was chosen for further examination in this study. Table 2 illustrates the number of fresh fuel assemblies, besides their ^{235}U enrichment levels, and labels (see Fig. 3a) of these assemblies for reaching 508 EFPDs within the design and operation limits.

Table 2
Number of fresh fuel assemblies and their enrichment level of 18-month cycle IFBA case.

Label	Number of fresh fuel assemblies	^{235}U enrichment (wt.%.)
C1	20	4.65
C2	16	4.70
C3	16	4.75
C4	12	4.80

Table 3 presents the required number of fuel assemblies as well as their ^{235}U enrichment levels, labels (see Fig. 3b), and the MDBAP and moderator radii to reach 1055 EFPDs for ZrB_2 MDBAP and UB_2 MDBAP scenarios.

The values of critical boron concentration, maximum Nuclear Enthalpy Rise Hot Channel Factor, Heat Flux Hot Channel Factor, burn-up and cycle EFPD for both the transition cycles and the equilibrium cycles utilizing both 18-month cycles with IFBAs and 36-month cycles with ZrB_2 MDBAPs as scenarios, are presented in Table 4. Additionally, the values for the same parameters utilizing UB_2 MDBAPs are presented in Table 5. In both Tables 4 and 5, the cycles labelled as "cycle 0″ were determined to be the final 18-month cycle with IFBA, while "cycle 1″ was determined to be the first 36-month cycle with MDBAP.

When 18-month and 36-month equilibrium cycles in Table 4 are examined, it is observed that the use of ZrB_2 MDBAP results in the need for ~27% lower initial critical boron concentration, 464 ppm, in the reactor core, despite the presence of a higher fissile isotope. This is attributed to the presence of the neutron absorber, ^{10}B in ZrB_2 MDBAP which decreases the need for initial boron concentration. Moreover, while utilizing ZrB_2 MDBAP in the 36-month equilibrium cycle results in a ~3.7% decrease in Nuclear Enthalpy Rise Hot Channel Factor in comparison to the 18-month equilibrium cycle using IFBA, there is a ~3.2% increase in the Heat Flux Hot Channel Factor.

When it comes to UB_2 MDBAP, on the other hand, the use of UB_2 MDBAP results in the need for ~34% lower initial critical boron concentration, 573 ppm, in the reactor core, despite the presence of a higher fissile isotope. This is also related to the high neutron absorber content of the design. Additionally, while utilizing UB_2 MDBAP in the 36-month Equilibrium cycle results in a ~3.8% decrease in Nuclear Enthalpy Rise Hot Channel Factor in comparison to the 18-month Equilibrium cycle using IFBA, there is a ~3.1% increase in the Heat Flux Hot Channel Factor.

Additionally, it has been observed that the utilisation of UB_2 MDBAP results in 1055 EFPDs with a lower burn-up rate (43.111 MWd/kgU for ZrB_2 and 42.291 MWd/kgU for UB_2 MDBAP). The attribution of this phenomenon is to the varying quantities of fissile material loaded due to the dimensional disparities between the necessary ZrB_2 and UB_2 MDBAPs, as well as the uranium content in UB_2. In addition, irrespective of the compound or material containing the uranium, the inherent fission characteristics of uranium remain consistent. This leads to a uniform burnup for an equivalent quantity of uranium and thus an equal amount of uranium loading into the reactor core will provide an equal amount of discharge burnup, depending on the type and amount of burnable absorber material within the core.

Figs. 6 and 7 show the Moderator Temperature Coefficient, Isothermal Temperature Coefficient, Uniform Doppler Coefficient, and Boron Coefficient curves for different equilibrium cycles. Specifically, while Fig. 6 shows the curves for an 18-month equilibrium cycle with IFBA, Fig. 7 a and b show the curves for 36-month equilibrium cycles with ZrB_2 and UB_2 MDBAPs, respectively.

During the IFBA equilibrium cycle, the uniform Doppler coefficient is initially measured at −1.43 pcm/°F. In contrast, at the beginning of the ZrB_2 MDBAP equilibrium cycle, it exhibits a value of −1.32 pcm/°F. Meanwhile, a shift is noticed in the boron coefficient, transitioning from −5.63 pcm/°F to −4.35 pcm/°F. On the other hand, in the UB_2 MDBAP equilibrium cycle, the uniform Doppler coefficient and boron coefficient

Table 3
Number of fresh fuel assemblies and their enrichment level and BA specifications of 36-month cycle MDBAP cases.

Label	Number of fresh fuel assemblies	ZrB_2 MDBAP			UB_2 MDBAP		
		^{235}U enrichment (wt. %)	Moderator radius (mm)	BA radius (mm)	^{235}U enrichment (wt. %)	Moderator radius (mm)	BA radius (mm)
C1	48	6.60	1.0	1.2	6.50	1.0	1.2
C2	33	6.65	0.9	1.3	6.55	1.1	1.5
C3	24	6.70	1.1	1.6	6.60	1.1	1.6
C4	24	6.75	1.1	1.3	6.65	0.9	1.2

Table 4
Equilibrium and transition cycles parameters of 18-month with IFBA and 36-month with ZrB_2 MDBAP cycles.

Cycle No.	Cycle Definition	CBC- BOC (ppm)	Maximum $F_{\Delta H}$	Maximum F_Q	Cycle Burn-up (MWd/kgU)	Cycle EFPD
−1	18-month Cycle (equilibrium)	1,687.4	1.616	1.948	19.925	507.8
0	18-month Cycle (equilibrium)	1,687.4	1.616	1.948	19.925	507.8
1	36-month transition cycle, first feed	1,242.1	1.530	1.983	42.655	1050.2
2	36-month transition cycle, second feed	1,224.0	1.555	2.009	43.137	1055.3
3*	36-month transition (equilibrium)	1,223.2	1.556	2.010	43.111	1054.7
4	36-month Cycle (equilibrium)	1,223.3	1.556	2.010	43.113	1054.7

Table 5
Equilibrium and transition cycles parameters of 18-month with IFBA and 36-month with UB_2 MDBAP cycles.

Cycle No.	Cycle Definition	CBC- BOC (ppm)	Maximum $F_{\Delta H}$	Maximum F_Q	Cycle Burn-up (MWd/kgU)	Cycle EFPD
−1	18-month Cycle (equilibrium)	1,687.6	1.616	1.948	19.925	507.8
0	18-month Cycle (equilibrium)	1,687.5	1.616	1.948	19.925	507.8
1	18-month transition cycle first feed	1,134.2	1.563	2.020	41.923	1050.1
2	36-month transition cycle second feed	1,115.8	1.527	2.007	42.318	1055.8
3*	36-month transition (equilibrium)	1,114.8	1.524	2.009	42.291	1055.1
4	36-month Cycle (equilibrium)	1,115.0	1.524	2.009	42.293	1055.2

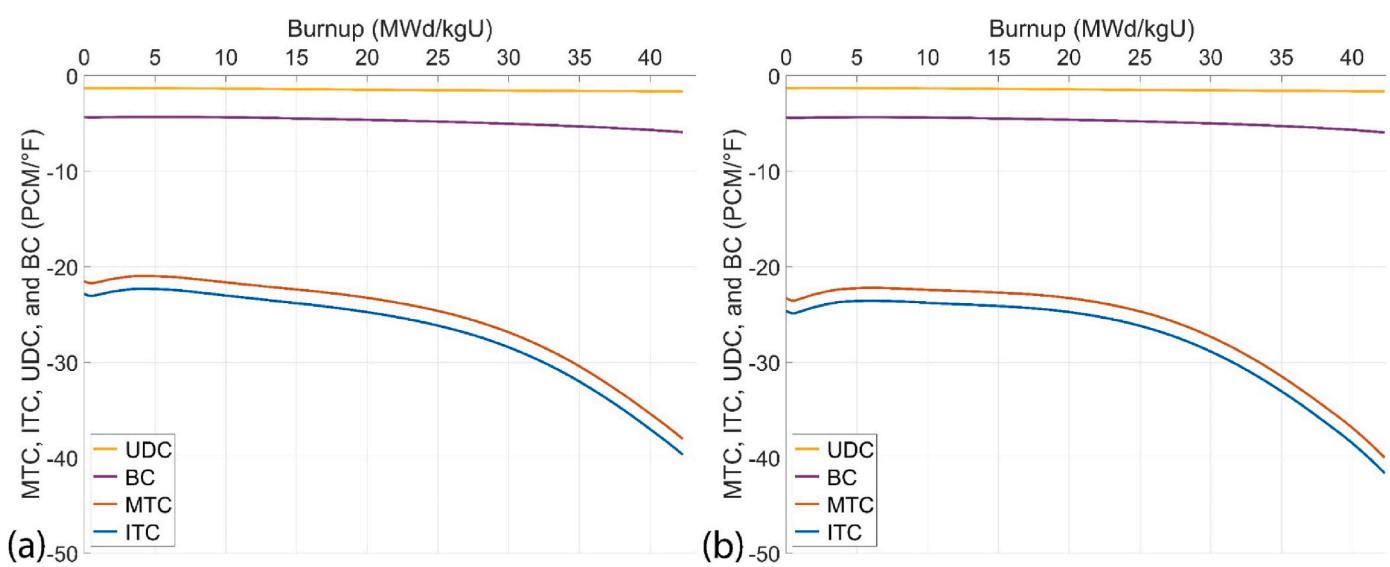

Fig. 7. Moderator temperature coefficient, isothermal temperature coefficient, uniform Doppler coefficient, and boron coefficient curves of 36-month equilibrium cycles with ZrB_2 MDBAP (a) and UB_2 MDBAP (b).

are noted at −1.31 pcm/°F and −4.41 pcm/°F, respectively.

For the IFBA equilibrium cycle, the recorded moderator temperature coefficient is −9.65 pcm/°F. However, in the ZrB_2 MDBAP equilibrium cycle, it is −21.52 pcm/°F, while it is −23.30 pcm/°F in the UB_2 MDBAP equilibrium cycle. These changes are attributed to the decreased boron content in the moderator. In addition, isothermal temperature coefficients for the IFBA and ZrB_2 MDBAP and UB_2 MDBAP equilibrium cycles are −11.06 pcm/°F, −22.85 pcm/°F and −24.63 pcm/°F, respectively. In addition, for both UB_2 and ZrB_2 equilibrium cycles', these parameters show similar values with the IFBA equilibrium cycle at

the end of the cycles. It is important to note that both the moderator temperature coefficient and the isothermal temperature coefficient remain within the designated design and operational limits throughout the cycles.

Upon examination of Figs. 6 and 7, it can be inferred that the utilisation of both ZrB_2 and UB_2 MDBAPs does not result in any negative impact on the moderator temperature coefficient, isothermal temperature coefficient, uniform Doppler coefficient, and boron coefficient values.

Table 6 shows the beginning and the end of the cycle SDM of the equilibrium cycles of IFBA, ZrB_2 MDBAP and UB_2 MDBAP.

Upon examination of Tables 6 and it is observed that in the 36-month cycle utilizing ZrB_2 MDBAP results in a decrease in SDM value of 1,423 pcm, approximately 42%, is observed at the beginning of the cycle in comparison to the 18-month cycle utilizing IFBA. Similarly, a reduction of 156 pcm, or approximately 7%, is observed at the end of the cycle. When the 36-month cycle utilizing UB_2 MDBAP is compared with the 18-month cycle utilizing IFBA, a reduction of 1,552 pcm, approximately 46%, is observed at the beginning of the cycle, and a reduction of 219 pcm, approximately 10%, observed at the end of the cycle. Furthermore, when comparing ZrB_2 with UB_2 MDBAPs, it can be seen that the UB_2 MDBAP equilibrium cycle has more negative SDM values than the ZrB_2 MDBAP equilibrium cycle in both at the beginning and the end of the cycle, with differences of approximately 7% and 3% respectively. The reduction in SDM within is related to the increasing quantity of fissile isotope present in the reactor core. Additionally, it is also attributed to the use of an absorber that has a relatively lower initial worth and is positioned inside the pellet. As a result, it is shielded by the fuel, unlike the IFBA placed outside the pellet, which is left unshielded and possesses an extremely high worth.

A great number of simulations were conducted to attain the desired EFPDs, in which a variation of ^{235}U enrichment level, and moderator and, MDBAP radii, yielding up to 1055 EFPDs was considered. Among the outcomes, higher SDM with UB_2 were also obtained in many cases, contrasting the values presented in Table 6. Consequently, it would be imprudent to infer the superiority of one over the other through a comparison between ZrB_2 and UB_2 MDBAPs, as the SDM value is greatly impacted by these parameters.

An examination of the average axial relative power fraction was conducted to evaluate the impact of the utilisation of MDBAP on the axial power distribution. Fig. 8 illustrates the average axial relative power fraction curves for the IFBA, ZrB_2 MDBAP and UB_2 MDBAP equilibrium cycles, at the beginning and end of the cycles.

When examining the average axial relative power fraction profiles, it was observed that in scenarios using ZrB_2 and UB_2 MDBAPs, very similar profiles were obtained both at the beginning of the cycle and the end of the cycle. When compared to the scenario using the 18-month IFBA, the difference between the minimum and maximum value at the beginning of the cycle decreases with the use of MDBAP, potentially resulting in a flatter profile trend. However, the profile at the end of the cycle has a plateau at the top region of the reactor in MDBAPs design which is different than the power profile of IFBA design that shows a flatter behaviour.

The assembly-wise differences in 2D relative power fractions between ZrB_2 MDBAP and UB_2 MDBAP were subject to analysis. Fig. 9 presents a comparison of the 2D relative power fractions of equilibrium cycles of ZrB_2 MDBAP and UB_2 MDBAP at the beginning (Fig. 9a) and end (Fig. 9b) of the cycles. An examination of assembly-wise 2D relative power fractions at the beginning of the cycle, as illustrated in Fig. 9a, revealed that variations within the range of +0.06 and −0.13 occurred on certain fresh fuel assemblies. Conversely, the assembly-wise differences in 2D relative power fractions at the end of the cycle were found to be quite minimal as anticipated in comparison to the beginning of the cycle, being within the range of +0.03 to −0.06.

Table 6
Shutdown Margin of IFBA, ZrB_2 MDBAP and UB_2 MDBAP equilibrium cycles.

Fuel Type	BOC (pcm)	EOC (pcm)
18-month cycle with IFBA	−3,368	−2,255
36-month cycle with ZrB_2 MDBAP	−1,945	−2,099
36-month cycle with UB_2 MDBAP	−1,816	−2,036

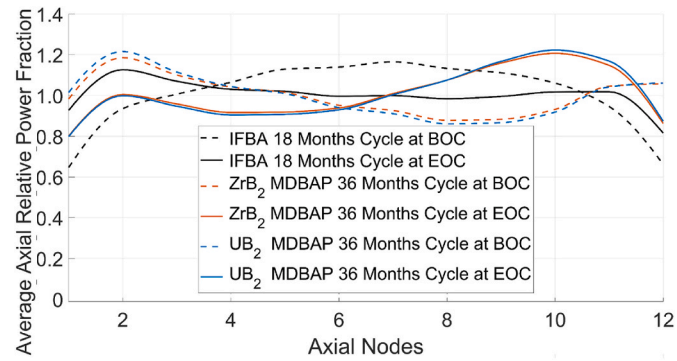

Fig. 8. Average axial relative power fraction curves of equilibrium cycles.

In general, with the use of MDBAP, it is possible to reach a 36-month cycle with a capacity factor of 96.3 from an 18-month cycle with a capacity factor of 92.7 within the design and safety limits. By this way, it is possible to decrease the planned outage period for refuelling over the given period. While the increased capacity factor brings more energy production, it will also bring economic advantages with operational flexibility in areas such as maintenance and handling of spent fuel.

5. Conclusions

- The use of beryllium oxide moderator and BA increase the production of fissile ^{239}Pu by hardening the neutron spectrum (Chen and Yuan, 2020; Sanders and Wagner, 2001). As a result, the consumption of ^{235}U atoms is reduced, leading to a higher burnup and longer cycle length.
- The presence of ^{235}U in UB_2 MDBAP adds a greater quantity of fissile isotopes within the reactor core. Thus, the enrichment of ^{235}U required to reach the same EFPD is lower in the case of UB_2 MDBAP compared to ZrB_2 MDBAP.
- Despite the high weight percent of ^{235}U used in 36-month cycles, this does not necessitate a high need for boron concentration. In fact, it contributes to reducing the required initial boron concentration. This highlights the potential of the MDBAP design to be employed in soluble boron-free reactor designs.
- The use of MDBAP reduces the maximum nuclear enthalpy rise hot channel factor while increases the heat flux hot channel factor.
- The use of MDBAPs causes no negative effects on parameters like the moderator temperature coefficient, isothermal temperature coefficient, uniform Doppler coefficient, and boron coefficient, ensuring safe and realistic operation.
- The shutdown margin in cases where MDBAP is used is reduced by the increased ^{235}U enrichment, however, the values obtained remain within the design and safety limits.
- By extending the cycle length from 18-month to 36-month, a higher capacity factor is achieved, leading to substantial economic benefits.

As the design under examination in this study is relatively novel, it is necessary to conduct appropriate experiments to verify the predictions and material selections. Additionally, future studies may assess the following points to reveal the unknowns of the design.

- Since the production of ^{4}He by the transmission of ^{10}B can increase the internal pressure, the effects of this under normal or beyond normal operating conditions should be investigated and, if necessary,

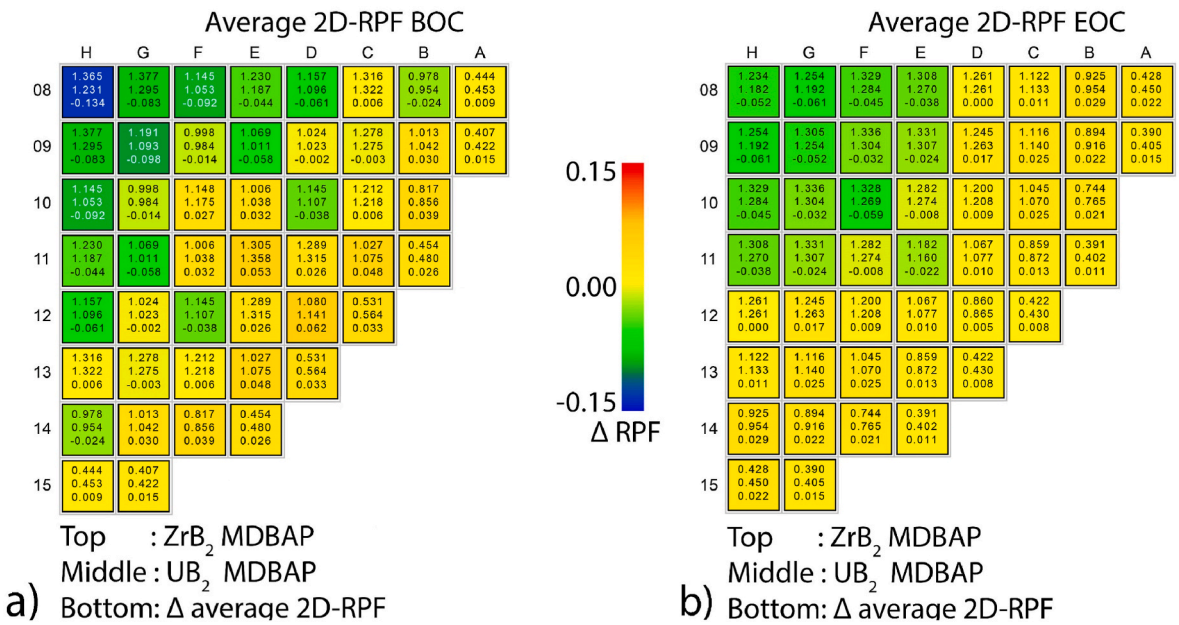

Fig. 9. Assembly-wise 2D relative power fraction profile of equilibrium cycles.

a design for evacuation should be considered or the use of non-He generating burnable absorbing materials (e.g. Gd/Gd-additive UO_2).

- The production costs of fuel pellets containing MDBAP should be determined and compared with IFBA, and the effect of the design on the levelized electricity cost of the front-end of the cycle should be investigated. In addition to this, the economic benefits that the design can provide should be revealed by analysing the differences that will arise on the back-end of the cycle with the transition from the 18-month to 36-month cycle.
- The material interactions between the MDBAPs and the annular UO_2 pellets must be evaluated to find out if the use of a barrier is necessary.
- The thermal properties of the design should be investigated with the finite element method.
- MDBAP behaviour during an accident or expected operational event should be investigated, considering the melting point, thermal expansion, and alterations in the specific heat capacity of the fuel.
- Exploration of the positioning of the BA at various lengths on the fuel rods can be carried out in order to achieve a flatter Axial relative power fraction profile, as the design is suitable for this.
- An optimization study should be conducted to achieve the targeted EFPD by obtaining the most uniform power profile and low peaking factor through the optimum MDBAP radius and moderator radius. Additionally, sensitivity analyses should be carried out to reveal the effects of changes in MDBAP and the moderator radii.
- An effective way to enhance SDM is by considering the IFBA as BA added to the MDBAP design which results in a hybrid IFBA/MDBAP design.
- It is necessary to investigate how essential maintenance outages are within this cycle and their influence on the overall economic costs. This research is critical to highlighting the importance of the economic feasibility of using MDBAPs.
- The testing of various sizes of MDBAPs can be performed with the aim of achieving a lower critical boron concentration, this could cause the shutdown margin to exceed the safety limits. In such a case, the optimization of control rods will be necessary.
- The modification of UB_2's uranium enrichment level in the utilisation of UB2 MDBAPs should be investigated as this might enhance the fuel's efficiency. Furthermore, research should be conducted employing the same uranium enrichment level to all UB_2 MDBAPs which will be loaded into the reactor core, as it might provide manufacturing advantages.
- In the MDBAP design, the performance of various materials can be tested to discover novel alternatives as moderators, thereby enabling the more efficient utilisation of fuel.

Declaration of competing interest

The authors declare that they have no known competing financial interests or personal relationships that could have appeared to influence the work reported in this paper.

Data availability

Data will be made available on request.

Acknowledgements

The authors would like to express their gratitude to the Republic of Turkey's Ministry of National Education. SCM and WEL are funded through the Sêr Cymru II programme by Welsh European Funding Office (WEFO) under the European Development Fund (ERDF).

References

Alameri, S.A., Alrwashdeh, M., 2021. Preliminary three-dimensional neutronic analysis of IFBA coated TRISO fuel particles in prismatic-core advanced high temperature reactor. Ann. Nucl. Energy 163, 108551. https://doi.org/10.1016/j.anucene.2021.108551.

Alhattawi, N.T., Alrwashdeh, M., Alameri, S.A., Alaleeli, M.M., 2023. Sensitivity neutronic analysis of accident tolerant fuel concepts in APR1400. J. Nucl. Mater. 582, 154487 https://doi.org/10.1016/j.jnucmat.2023.154487.

Alrwashdeh, M., Alameri, S.A., 2023. A neutronics study of the initial fuel cycle extension in APR-1400 reactors: examining homogeneous and heterogeneous enrichment design. Arabian J. Sci. Eng. https://doi.org/10.1007/s13369-023-07905-7.

Ames Ii, D.E., Tsvetkov, P.V., Rochau, G.E., Rodriguez, S., 2010. High fidelity nuclear energy system optimization towards an environmentally benign. Sustainable, and Secure Energy Source. https://doi.org/10.2172/992769.

Amjad, N., Hidekazu, Y., Ming, Y., 2014. Burnup study of 18 months and 16/20 months cycle AP1000 cores using CASMO4E and SIMULATE-3 codes. Nucl. Saf. Simul. 5.

Attom, A.M., Wang, J., Yan, C., Ding, M., 2019. Neutronic analysis of thorium MOX fuel blocks with different driver fuels in advanced block-type HTRs. Ann. Nucl. Energy 129, 101–109. https://doi.org/10.1016/j.anucene.2019.01.049.

Barsic, J.A., Conner, M.E., Everhard, A.M., Grover, J.L., Huegel, D.S., Keiser, K.E., Monahan, E.M., Neubert, K.B., Nissley, M.E., Risher, D.H., Schoff, R.R., Secker, J.R., Sung, Y.X., 2008. WCAP-16498-NP,17x17 Next Generation Fuel (17x17 NGF) Reference Core Report.

Berglund, M., Wieser, M.E., 2011. Isotopic compositions of the elements (IUPAC technical report). Pure Appl. Chem. 83, 397–410. https://doi.org/10.1351/PAC-REP-10-06-02.

Bolukbasi, M.J., Middleburgh, S.C., Lee, W.E., 2023. In-reactor behaviour and economic assessment of enriched gadolinia burnable absorbers. Prog. Nucl. Energy 164, 104873. https://doi.org/10.1016/j.pnucene.2023.104873.

Bolukbasi, M.J., Middleburgh, S.C., Vrtiska, S., Lee, W.E., 2022. Effect of ZrB2 and UB2 discrete burnable absorber pins on fuel reactivity. Prog. Nucl. Energy 150, 104295. https://doi.org/10.1016/j.pnucene.2022.104295.

Burr, P.A., Kardoulaki, E., Holmes, R., Middleburgh, S.C., 2019. Defect evolution in burnable absorber candidate material: uranium diboride, UB2. J. Nucl. Mater. 513, 45–55. https://doi.org/10.1016/j.jnucmat.2018.10.039.

Carelli, M.D., Ingersoll, D.T., 2014. Handbook of small modular nuclear reactors. Handbook of Small Modular Nuclear Reactors. https://doi.org/10.1016/C2013-0-16379-9.

Carlson, L., Wu, Z., Olson, J., Liu, L., Emily, 2020. An economic cost assessment on HALEU fuels for small modular reactors. Sci. Technol. Nucl. Install. https://doi.org/10.1155/2020/8815715, 2020.

Chen, S., Yuan, C., 2020. Neutronic study of UO2-BeO fuel with various claddings. Nucl. Mater. Energy 22.

Choe, J., Shin, H.C., Lee, D., 2016. New burnable absorber for long-cycle low boron operation of PWRs. Ann. Nucl. Energy 88, 272–279. https://doi.org/10.1016/j.anucene.2015.11.011.

Dalle, H.M., Mattos, J.R.L. de, Dias, M.S., 2013. Enriched gadolinium burnable poison for PWR fuel – Monte Carlo burnup simulations of reactivity. In: Current Research in Nuclear Reactor Technology in Brazil and Worldwide. https://doi.org/10.5772/53381.

Dandi, A., Lee, M.J., Kim, M.H., 2020. Feasibility of combinational burnable poison pins for 24-month cycle PWR reload core. Nucl. Eng. Technol. 52, 238–247. https://doi.org/10.1016/J.NET.2019.07.026.

Dias, M.S., de Mattos, J.R.L., de Andrade, E.P., 2019. Very high burnup fuel for Angra 2 NPP within the 5 w/o limit of the 235 U-enrichment. Nucl. Eng. Des. 346, 17–23. https://doi.org/10.1016/j.nucengdes.2019.02.023.

DiGiovine, A.S., Gheorghiu, H.-N.M., 1999. Generic CMS PWR Equilibrium Model Revision 3.

Duke, Energy, 2018. Harris Nuclear Power Plant Core Operating Limits Report.

Durazzo, M., Freitas, A.C., Sansone, A.E.S., Ferreira, N.A.M., de Carvalho, E.F.U., Riella, H.G., Leal Neto, R.M., 2018. Sintering behavior of UO2–Er2O3 mixed fuel. J. Nucl. Mater. 510, 603–612. https://doi.org/10.1016/j.jnucmat.2018.08.051.

Elsawi, M.A., Hraiz, A.S.B., 2015. Benchmarking of the WIMS9/PARCS/TRACE code system for neutronic calculations of the Westinghouse AP1000^{TM} reactor. Nucl. Eng. Des. 293, 249–257. https://doi.org/10.1016/j.nucengdes.2015.08.008.

Enica, A., Middleburgh, S.C., Vrtiska, S.J., 2018. Annular Nuclear Fuel Pellets with Discrete Burnable Absorber Pins. US2018330832A1.

Evans, J.A., DeHart, M.D., Weaver, K.D., Keiser, D.D., 2022. Burnable absorbers in nuclear reactors – a review. Nucl. Eng. Des. 391, 111726 https://doi.org/10.1016/J.NUCENGDES.2022.111726.

Garcia-Delgado, L., Driscoll, M.J., Meyer, J.E., Todreas, N.E., 1999. An Economically Optimum PWR Reload Core for a 36-month Cycle 26.

Hiscox, B., 2018. Analysis and Optimization of a New Accident Tolerant Fuel Called Fuel-In-Fibers. Massachusetts Institute of Technology.

IAEA, 2020. Advances in small modular reactor technology developments. A Suppl. to IAEA Adv. React. Inf. Syst, 2020 Ed. 354.

Insulander Björk, K., Kekkonen, L., 2015. Thermal-mechanical performance modeling of thorium-plutonium oxide fuel and comparison with on-line irradiation data. J. Nucl. Mater. 467, 876–885. https://doi.org/10.1016/j.jnucmat.2015.11.001.

Kardoulaki, E., White, J.T., Byler, D.D., Frazer, D.M., Shivprasad, A.P., Saleh, T.A., Gong, B., Yao, T., Lian, J., McClellan, K.J., 2020. Thermophysical and mechanical property assessment of UB2 and UB4 sintered via spark plasma sintering. J. Alloys Compd. 818, 153216 https://doi.org/10.1016/j.jallcom.2019.153216.

Lokhov, A., Cameron, R., Sozoniuk, V., 2013. OECD/NEA study on the economics and market of small reactors. Nucl. Eng. Technol. 45, 701–706. https://doi.org/10.5516/NET.02.2013.517.

Papynov, E.K., Shichalin, O.O., Belov, A.A., Portnyagin, A.S., Buravlev, I.Y., Mayorov, V. Y., Sukhorada, A.E., Gridasova, E.A., Nomerovskiy, A.D., Glavinskaya, V.O., Tananaev, I.G., Sergienko, V.I., 2020. Spark plasma sintering of UO2 fuel composite with Gd2O3 integral fuel burnable absorber. Nucl. Eng. Technol. 52, 1756–1763. https://doi.org/10.1016/j.net.2020.01.032.

Qin, M.J., Middleburgh, S.C., Cooper, M.W.D., Rushton, M.J.D., Puide, M., Kuo, E.Y., Grimes, R.W., Lumpkin, G.R., 2020. Thermal conductivity variation in uranium dioxide with gadolinia additions. J. Nucl. Mater. 540, 152258 https://doi.org/10.1016/j.jnucmat.2020.152258.

Renier, J.-P.A., Grossbeck, M.L., 2001. Development of Improved Burnable Poisons for Commerical Nuclear Power Reactors.

Sanders, C.E., Wagner, J.C., 2001. Impact of Integral Burnable Absorbers on PWR Burnup Credit Criticality Safety Analyses. NCSD Conference Paper.

Stewart, R., Blakely, C., Zhang, H., 2021. Investigation of a two-year cycle pressurized water reactor core design with increased enrichment and extended burnup limits. Nucl. Eng. Des. 376, 111132 https://doi.org/10.1016/J.NUCENGDES.2021.111132.

U.S.NRC, 1982. Technical Specifications, Virgil C. Summer Nuclear Station.

Westinghouse Electric Company, 2018. Nuclear Fuel - Integral Fuel Burnable Absorber (IFBA) Fuel Cycles and IFBA/Gad Hybrid Fuel Cycles.

World Nuclear Association, 2021. Nuclear Fuel and its Fabrication [WWW Document]. https://world-nuclear.org/information-library/nuclear-fuel-cycle/conversion-enrichment-and-fabrication/fuel-fabrication.aspx.